1 October 2001

ELSEVIER

Optics Communications 197 (2001) 475–480

OPTICS COMMUNICATIONS

www.elsevier.com/locate/optcom

Characteristics of the oscillatory spectrum due to only induced-phase modulation in an argon-filled hollow waveguide accompanied with intense self-phase modulation

Naoki Karasawa [a,*], Ryuji Morita [a], Hidemi Shigekawa [b], Mikio Yamashita [a]

[a] *Department of Applied Physics, Hokkaido University, Core Research for Evolutional Science and Technology, Japan Science and Technology Corporation, Kita-13, Nishi-8, Kita-Ku, Sapporo 060-8628, Japan*

[b] *Institute of Applied Physics, University of Tsukuba, Core Research for Evolutional Science and Technology, Japan Science and Technology Corporation, 1-1-1 Tennodai, Tsukuba 205-8573, Japan*

Received 18 December 2000; received in revised form 18 July 2001; accepted 19 July 2001

Abstract

We experimentally observed the periodic oscillatory structure in the second-harmonic spectrum when we simultaneously propagated intense fundamental and second-harmonic pulses from a Ti:sapphire laser-amplifier system in an argon-filled capillary fiber. The periodic oscillatory structure in the second-harmonic spectrum is only due to the induced-phase modulation (IPM) which, in general, is hidden because of strong self-phase modulation. It is found that this structure can be well explained by the interference of the electric field components in the second-harmonic pulse. These electric field components are generated based on IPM by the fundamental pulse. The theoretical analysis of the nonlinear pulse propagation agrees well with experimental results. In addition, the measured dependence of the modulated spectral behavior on the delay time, including the spectral feature, the oscillatory period and the range of the delay time between two pulses, indicates the excellent agreement with the numerical analysis which includes the medium and waveguide dispersion and the steepening effect.

Keywords: Induced-phase modulation (IPM); Self-phase modulation (SPM); Capillary fiber; Nonlinear pulse propagation

1. Introduction

When an intense optical pulse is propagated in an optically nonlinear medium, self-phase modulation (SPM) occurs. The phase of the pulse is modulated because of the intensity-dependent change of the refractive index of the medium, and the spectrum of the pulse is broadened by chirp arising from this temporal change of the phase. It is well known that the periodic oscillatory structure in the spectrum arises from SPM [1]. This periodic structure can be explained from the interference between the intra-pulse electric fields with the identical frequencies separated in time [2]. The number of peaks in the structure gives the estimate of the phase shift induced by the pulse intensity. Recently, we have applied the induced-phase

* Corresponding author. Present address: Department of Applied Photonics System Technology, Chitose Institute of Science and Technology, 758-65 Bibi, Chitose 066-8655, Japan. Fax: +81-123-27-6063.

E-mail address: n-karasa@photon.chitose.ac.jp (N. Karasawa).

0030-4018/01/$ - see front matter
PII: S0030-4018(01)01456-0

modulation (IPM) effect [3,4] to generate ultrabroadband optical pulses in a fused-silica fiber [5–7] and in a capillary fiber filled with argon [8]. This IPM is also known as cross-phase modulation (XPM) [1]. (However in Ref. [3], XPM is specifically used to represent the phase modulation and change of emission spectrum caused by the interference between stimulated Raman scattering and SPM.) In the capillary fiber experiments, both intense fundamental and second-harmonic pulses from a Ti:sapphire laser-amplifier system were copropagated. The intensity of both pulses was about the same and the phase modulation of one pulse was induced by the other pulse (IPM) in addition to that due to its own pulse (SPM). As a result, the coherent pulse with the bandwidth exceeding one octave (300–1000 nm) has been generated [8], which is essential for the successful achievement of monocycle pulses to be generated after chirp compensation covering the entire frequency range. However, the detailed mechanism of the complicated structure in the modulated spectrum in the case that the IPM and SPM effects coexist in the almost same magnitude has not been revealed, and its clarification is significantly important for complete chirp compensation.

In this paper, we clarify through theoretical and experimental observation the origin of the complicated oscillatory structure in the spectrum under intense induced- and self-phase modulations in an argon-filled capillary fiber by controlling precisely the delay time between two pulses. Furthermore, it is shown that the observed IPM-induced spectral behavior excellently agrees with the numerical results of the theoretical analysis.

2. Experiment

The experimental setup is shown in Fig. 1, which is similar to the apparatus used by Karasawa et al. [8]. The output beam of a Ti:sapphire laser-amplifier system (Femtopower 1000; center wavelength $\sim$ 790 nm; pulse width 32 fs; repetition rate, 1 kHz; pulse energy, 1 mJ) was separated by a beam splitter (BS), which reflected 30% of pulse energy. The transmitted beam was passed through a 0.5-mm-thick β-barium borate (BBO) crystal.

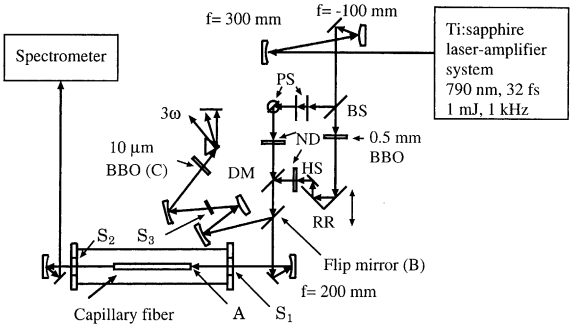

Fig. 1. Experimental setup. See text for definitions.

The delay of the generated second-harmonic pulse was adjusted by a retroreflector (RR) and separated by a harmonic separator (HS). The polarization direction of the fundamental beam was rotated by 90° using two periscopes (PS) to match it with that of the second-harmonic beam. Neutral density filters (ND) were used to adjust the intensities of both beams. Two beams were combined by a dichroic mirror (DM) and focused at the input end of the fiber (A), which was positioned inside a chamber filled with an argon gas with a pressure of 2.8 atm. The chamber had two 1-mm-thick sapphire windows (S_1 and S_2). The capillary fiber was made of fused silica, and its length and inner diameters were 34 cm and 0.1 mm, respectively. To determine the delay time of the second-harmonic pulse relative to the fundamental pulse (T_{d2}), the combined beam was redirected by a flip mirror (B), passed through 1-mm-thick sapphire plate (S_3), and focused at a 10-μm-thick BBO crystal (C) to generate the sum-frequency signal. The optical distance between the flip mirror (B) and the BBO crystal (C), and that between the flip mirror (B) and the input end of the fiber (A), were set to be equal by inserting an extra sapphire plate (S_3) and by taking into account of the dispersion of the argon and air [8]. The delay time that gave the maximum sum-frequency signal corresponded to the case for which both pulses met at the fiber input end (A) ($T_{d2} = 0$). When it was negative, the second-harmonic pulse entered the fiber before the fundamental pulse did. Input pulse energies were 40.8 μJ for fundamental and 27 μJ for second-harmonic pulses and output pulse energies were 15.5 μJ for fundamental and 10.5 μJ for second-

harmonic pulses, respectively. The temporal widths of the input pulses were measured by a transient-grating frequency-resolved optical gating apparatus [9]. They were found to be 32 and 72 fs for fundamental and second-harmonic pulses, respectively. The peak powers for the pulses were 1.28 GW for fundamental and 0.377 GW for second harmonic, and the center wavelengths were 790 nm for fundamental and 405 nm for second-harmonic pulses.

The spectra observed for the second-harmonic pulse are shown in Fig. 2. In Fig. 2(a), the delay time ($T_{d2} = -207$ fs) was selected such that both pulses did not overlap inside a fiber. In this case, the IPM spectrum (solid curve) was almost identical to the SPM spectrum (dotted curve, measured for the propagation of only the second-harmonic pulse). This showed the oscillatory structure with a period of ~20 THz in the high frequency region. When the delay time T_{d2} was increased (Fig. 2(b)–(d)), pulses began to overlap inside a fiber, and a new oscillatory structure with the shorter period of ~10 THz in the low frequency region was observed as indicated by arrows. As the overlap increased, this new structure became more pronounced. For the even larger delay time T_{d2} (Fig. 2(e)), the overlap between fundamental and second-harmonic pulses became large such that the original SPM spectrum shape was modified considerably. Although the oscillatory structure was still present in this case, the strong modification of the main spectrum by SPM made the identification of IPM oscillation difficult.

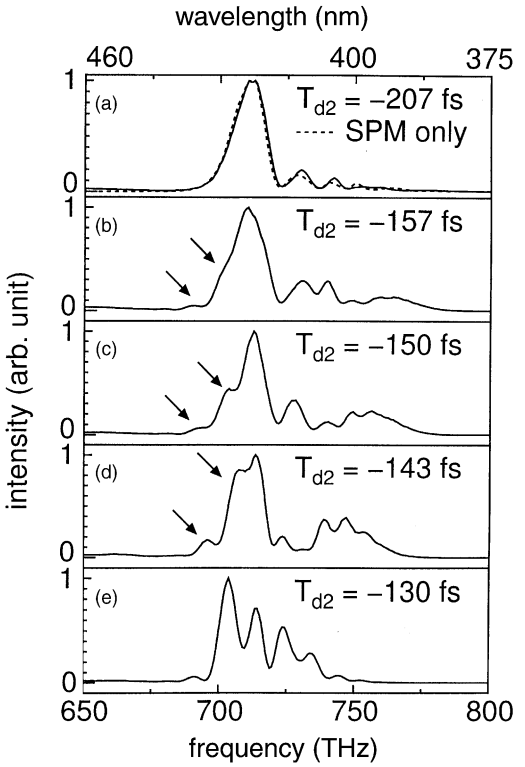

Fig. 2. Experimental spectra where both fundamental and second-harmonic pulses were co-propagated in an argon-filled capillary fiber with different delay times (a–e). Oscillatory structure due to only IPM is indicated by arrows. In (a), the spectrum where only second-harmonic pulses were propagated is shown by a dotted line.

3. Comparison with theory

Since the dispersion length of a capillary fiber is much longer than the nonlinear length in this case, the dispersion effect can be ignored in the first approximation. We have used the exact solution of chirps for Gaussian input pulses for a dispersionless waveguide with a loss [10]. In Fig. 3, the instantaneous frequency $\delta\nu_2$ ($= \delta\omega_2/2\pi$: nonlinear chirp) for the second-harmonic pulse (at $z_l =$ 34 cm) is shown with the relative position of two pulses for different delay times used in the experiments. The nonlinear chirp at the position z_l, $\delta\omega_2(z_l, T_2)$ is given by

$$\delta\omega_2(z_l, T_2) = \frac{2n_2\omega_2}{cA}\frac{z_l}{T_{02}}\left[\frac{z_{2\mathrm{eff}}}{z_l}(\tau_2' - \tau_{d2})\exp[-(\tau_2' - \tau_{d2})^2]P_2 - \frac{1}{\delta_2}\exp(2\eta_1\tau_1' + \eta_1^2)P_1\sqrt{\pi}\eta_1\{\mathrm{erf}(\tau_1' + \eta_1 + \delta_1) - \mathrm{erf}(\tau_1' + \eta_1)\} - \frac{1}{\delta_2}\exp(2\eta_1\tau_1' + \eta_1^2)P_1 \times \left\{\exp[-(\tau_1' + \eta_1 + \delta_1)^2] - \exp[-(\tau_1' + \eta_1)^2]\right\}\right]. \quad (1)$$

Here, the input envelope for the fundamental pulse ($i = 1$) is given by $A_1(0, T_1) = \sqrt{P_1}\exp[-T_1^2/(2T_{01}^2)]$ and that of the second-harmonic pulse ($i = 2$) is given by $A_2(0, T_2) = \sqrt{P_2}\exp[-(T_2 - T_{d2})^2/(2T_{02}^2)]$

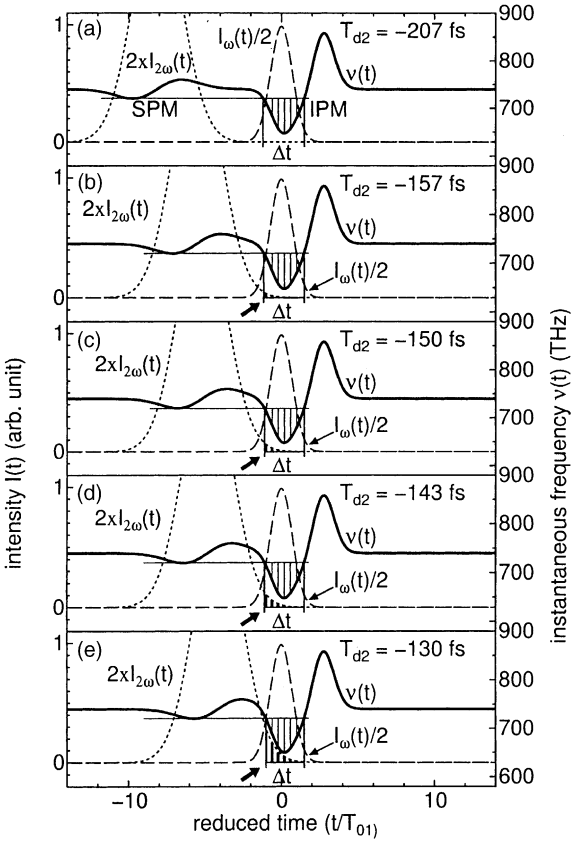

Fig. 3. Calculated instantaneous frequencies $v(t)$ (solid line) and the intensities $I_{2\omega}(t)$ (dotted line) of the second-harmonic pulse and the intensities I_ω at the fiber output at different delay times. Thin horizontal lines show the minimum instantaneous frequency created by SPM. The instantaneous frequencies and the intensities of second-harmonic pulses in the temporal region where the instantaneous frequencies are created twice due to only IPM are hatched by thin lines and thick lines, respectively. Gaussian input pulses are assumed and the dispersion and the steepening effects are neglected. See text for input parameters.

in the time coordinates T_i moving at group velocities v_{gi}, where P_i is the peak power, T_{0i} is the pulse width (full-width-at-half-maximum-width divided by 1.665), and T_{d2} is the delay time of the second-harmonic pulse relative to the fundamental pulse. The parameters n_2, ω_2, c, and A are the nonlinear index of refraction (2.744×10^{-23} m^2/W [8]), the center angular frequency of the second-harmonic pulse ($2\pi c/(405\text{ nm})$), the speed of light, and the cross-section of the capillary fiber (πa^2, $a =$ 50 μm). $z_{2\text{eff}} = (1 - \exp(-\alpha_2 z_l))/\alpha_2$ is the effective length of the fiber for the second-harmonic pulse with the loss $\alpha_2 = 0.568$ m^{-1}. Also, the normalized parameters are defined as $\tau_i' = T_2/T_{0i}$, $\tau_{d2} = T_{d2}/T_{02}$, $\delta_i = z_l d/T_{0i}$, and $\eta_1 = \alpha_1 T_{01}/2d$ with $\alpha_1 = 2.16$ m^{-1}. d is the difference of the inverse group velocities of pulses, and is given by $d = 1/v_{g2} - 1/v_{g1} = 150$ fs/m. The first term of Eq. (1) shows the chirp arising from SPM. The second and third terms arise from IPM. The second term arises from the phase change of the second-harmonic pulse induced by the shape change of the fundamental pulse due to its loss during propagation. The third term arises mainly from the imperfect overlap of both pulses at fiber ends [10]. The second term is insignificant for the present experimental condition because the loss is small.

As shown in Fig. 3, the spectral components for the second-harmonic pulse whose frequency is lower than the center frequency (740 THz) are created by both SPM and IPM. However, it is found that the spectral components less than the minimum frequency created by SPM (~720 THz, indicated by thin horizontal lines in Fig. 3) are created only by IPM from the intense fundamental pulse (which is described by the third term of Eq. (1)) and these frequencies are created twice at different times (hatched by thin lines in Fig. 3). The novel oscillatory structure in the spectrum appears because of the interference between these two electric field components with the identical instantaneous frequencies by IPM. When the delay is sufficiently negative (Fig. 3(a)), the intensity of the second-harmonic pulse $I_{2\omega}(t)$ in this region is essentially zero, so that the interference is not observed. When the delay times become less negative (Fig. 3(b)–(d)), the intensity in this region (hatched by thick lines) becomes stronger and the interference patterns can be observed. When the delay becomes even less negative (Fig. 3(e)), the chirps due to SPM and IPM in the region from 675 to 775 THz are becoming similar in magnitude because of the large intensity of the pulse and the interference pattern shown here becomes difficult to identify.

In Fig. 4, the spectra calculated by numerically solving the nonlinear fiber propagation equation at the same delay times as in the experiment are shown. In these calculations, the dispersion of the gas medium and the waveguide (including loss

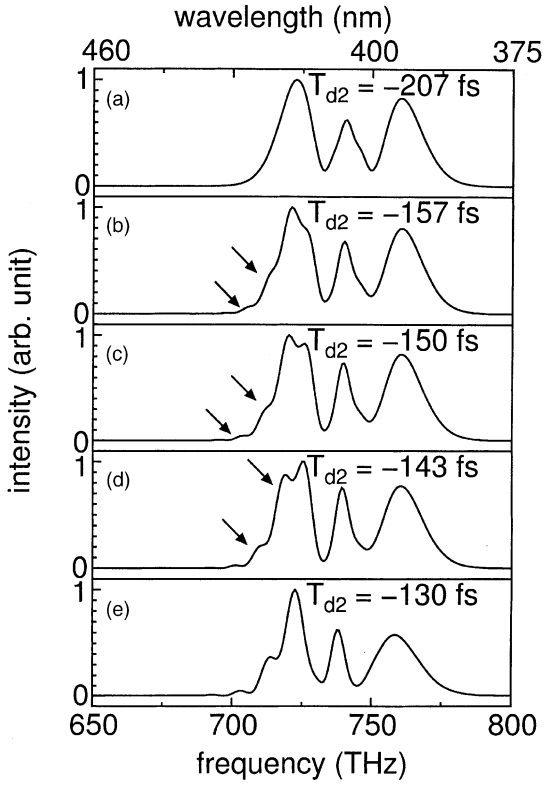

Fig. 4. Numerically calculated spectra at the same delay time for the same input parameters as shown in Fig. 3. In calculations, the gas as well as the waveguide dispersions and the steepening effect were taken into account.

dispersion) was rigorously included, and the steepening effect was taken into account [11]. As shown in Fig. 4, the clear oscillatory structure in the low frequency region, as observed in the experiment for cases (b)–(d), was obtained. The spectral feature, the oscillatory period (~10 THz) and the delay-time range show the excellent agreement with the experimental results. This clearly demonstrates that Eq. (1) is valid in the current experimental situation. At the largest negative delay time (a), the oscillatory structure as in (b)–(d) was not observed. At the smallest negative delay time (e), even though the oscillatory structure was observed, the original SPM structure was strongly modified, as clearly indicated by the suppression of the peak at 765 THz. The detailed shapes of spectra did not agree quantitatively with experimental ones mainly due to differences of initial pulse shapes. In calculations, Gaussian input pulses were assumed. On the other hand, small deviations from Gaussian pulses were observed in experiments. Moreover, small side pulses were observed for fundamental pulses. These should be responsible for the differences of detailed shapes of second-harmonic spectra between calculations and experiments.

4. Conditions for observing IPM-only oscillation

From the previous results of comparisons between experiment and theory, the conditions to observe IPM-only-induced spectral oscillations can be determined. First, to observe the visible fringes, we need to have sufficient intensity for the second-harmonic pulse at which chirp from IPM is present. This limits the upper bound of the temporal separation between the two pulses. For cases treated here, the loss is small ($\eta_i \simeq 0.1$), thus the second term in Eq. (1) can be neglected. The IPM negative chirp is given by the last term in Eq. (1). This term becomes most negative near $\tau_1' + \delta_1 = 0$ or equivalently, $\tau_2' = -\delta_2$. The intensity of the second-harmonic pulse is proportional to $\exp[-(\tau_2' - \tau_{d2})^2]$. By requiring its intensity at $\tau_2' = -\delta_2$ to be more than 10^{-4} of its peak value to observe the fringe, we obtain the condition, $\tau_{d2} > -4.22$ or $T_{d2} > -181$ fs. This implies that the separation between two pulses should be less than 181 fs to observe the fringe. This agrees well with the experiments where the fringes were observed at $T_{d2} > -160$ fs. Second, to observe the clear oscillation due to *only* IPM, the SPM chirp should not be influenced by the IPM chirp too much. The chirp arising from SPM is given by the first term in Eq. (1), which is positive for $\tau_2' > \tau_{d2}$. When the separation of both pulses becomes small, this positive chirp from SPM is partly canceled by the negative chirp from IPM, which is again given by the last term in Eq. (1). For the small loss, $z_{2\text{eff}} \simeq z_l$ and the first term in the bracket in Eq. (1) becomes $P_2(\tau_2' - \tau_{d2})\exp[-(\tau_2' - \tau_{d2})^2]$. This term has the maximum value of $0.429P_2$ at $\tau_2' - \tau_{d2} = 1/\sqrt{2}$ and has the half-maximum value of $0.214P_2$ at $\tau_2' - \tau_{d2} = 1.36$. If we consider the case where the positive SPM chirp is canceled by the negative IPM

chirp at this half-maximum time, we can determine τ_{d2} from the condition $0.214P_2 = (P_1/\delta_2) \times \exp[-(\tau_1' + \delta_1)^2]$. The last relationship is obtained from the first and last terms in Eq. (1) where $\tau_1' = \tau_2' T_{02}/T_{01}$. In the present case, using $\tau_2' = 1.36 + \tau_{d2}$ in the above equation, we obtain $\tau_{d2} = -3.26$ or $T_{d2} = -140$ fs. Thus, if the temporal separation between two pulses becomes less than 140 fs, the SPM chirp is strongly influenced by the IPM, and hence the SPM spectrum will be strongly modified, which makes the identification of the interference pattern due to only IPM difficult. In the experimental results, when the separation time was less than about 130 fs, the original SPM spectrum was modified so strongly that clear fringes by IPM were not observed. This agrees well with the above estimate.

Thus from the theoretical estimate, the fringe pattern due to *only* from IPM can be clearly identified when $-3.26 > \tau_{d2} > -4.22$ or $-140 > T_{d2} > -181$ fs, which agrees well with the experimental results.

5. Conclusion

The novel oscillatory structure in second-harmonic spectrum due to only IPM was observed when we co-propagated fundamental and second-harmonic pulses in an argon-filled single mode capillary fiber. The analytic solutions without dispersion indicate definitely that it is indeed arising from the interference between the identical frequency components created only by IPM, and it was confirmed by the numerical calculations including the rigorous dispersion and the steepening effects. By using the simple analyses, we can estimate the range of the delay time between two pulses, in which we can clearly identify the interference pattern due to *only* IPM. Conversely, it is expected that by measuring in this range, the quantitative information regarding the pulse shape, the phase dispersion and the strength of the IPM effect in the nonlinear medium can be extracted. Moreover, these results suggest that the capillary fiber is an ideal nonlinear medium to clarify the complicated dynamic mechanism of the IPM chirp because it provides the small dispersion, the small nonlinear refractive index, the small loss and the well-controlled beam diameters.

References

[1] G.P. Agrawal, Nonlinear Fiber Optics, Academic, San Diego, CA, 1989.
[2] R. Cubeddu, R. Polloni, C.A. Sacchi, O. Svelto, Phys. Rev. A 2 (1970) 1955–1963.
[3] R.R. Alfano, P.P. Ho, IEEE J. Quant. Electron. 24 (1988) 351–364.
[4] P.L. Baldeck, P.P. Ho, R.R. Alfano, in: R.R. Alfano (Ed.), The Supercontinuum Laser Source, Springer, Berlin, 1989, pp. 117–183.
[5] M. Yamashita, H. Sone, R. Morita, Jpn. J. Appl. Phys. 35 (1996) L1194–L1197.
[6] M. Yamashita, H. Sone, R. Morita, H. Shigekawa, IEEE J. Quant. Electron. 34 (1998) 2145–2149.
[7] L. Xu, N. Karasawa, N. Nakagawa, R. Morita, H. Shigekawa, M. Yamashita, Opt. Commun. 162 (1999) 256–260.
[8] N. Karasawa, R. Morita, H. Shigekawa, M. Yamashita, Opt. Lett. 25 (2000) 183–185.
[9] J.N. Sweetser, D.N. Fittinghoff, R. Trebino, Opt. Lett. 22 (1997) 519–521.
[10] N. Karasawa, R. Morita, L. Xu, H. Shigekawa, M. Yamashita, J. Opt. Soc. Am. B 16 (1999) 662–668.
[11] N. Karasawa, S. Nakamura, N. Nakagawa, M. Shibata, R. Morita, H. Shigekawa, M. Yamashita, IEEE J. Quant. Electron. 37 (2001) 398–404.